

Nanocrystalline mesoporous zeolite X with a considerable external surface area prepared via an ordered precursor: a potential adsorbent

Xu Wang, Bin Yang, Jinghong Ma , Chunfeng Fen, Ruifeng Li

Institute of Special Chemicals, College of Chemistry and Chemical Engineering, Taiyuan University of Technology, Taiyuan 030024, People's Republic of China

✉ E-mail: majinghong@tyut.edu.cn

Published in Micro & Nano Letters; Received on 24th May 2016; Accepted on 20th July 2016

A nanocrystal zeolite X with intracrystalline mesopores has been successfully prepared by using organofunctionalised mesoporous silica in hydrothermal system. The as-prepared zeolitic material persist the inherent framework structure of FAU zeolite, and present a crystallographic morphology of stacked three-dimensional intergrowths made up of rectangular nanocrystals. The intracrystalline mesopores are formed via a bond-blocking principle with hydrophobic carbon chains of organosilane inhibiting the growth of zeolite units and crystals in the channels of mesoporous silica during hydrothermal synthesis. The results showed that the zeolitic material has a considerable external surface area ($247\text{ m}^2\text{g}^{-1}$) and mesopore volume ($0.44\text{ cm}^3\text{g}^{-1}$), maintaining high Brunauer–Emmett–Teller surface area ($991\text{ m}^2\text{g}^{-1}$) and large total pore volume ($0.71\text{ cm}^3\text{g}^{-1}$), and clearly stating a larger adsorption capacity for p-xylene at relative higher pressure.

1. Introduction: Zeolite is a crystalline aluminosilicate with regular, microscopic pores and windows of molecular dimensions (usually $<1.0\text{ nm}$), and desirable in molecular sieve, adsorbent and catalyst [1, 2]. However, intrinsic problems of zeolites are the inability of large molecules to accesses into the inner zeolite channel network and restriction of the mass transport in the micropores of zeolites, which undermines the effectiveness and fields of applications for zeolites [3]. To overcome this diffusion limitation, one of the more generally applied strategies to obtain materials with sufficient molecular transport properties is the creation of a so-called ‘hierarchical pore structure’ [4] by introducing a secondary pore system consisting of mesoporous (2–50 nm) inside the microporous zeolite crystals, which should have additional intra or intercrystalline mesoporosity in addition to the inherent microporosity of zeolites.

The synthesis of hierarchical porous materials has received much attention in the past decades [5, 6]. Zeolite crystals with additional meso (or in few cases macro) pores can be produced by different methods [7], such as, desilication by an alkaline post-treatment [8, 9] or by the use of hard [10, 11] and soft [12–14] templates during zeolite synthesis. However, all the methods are usually limited to a certain group of zeolites or just to a special zeolite type. For high-silica zeolites, such as ZSM-5, several methods for incorporating additional transport pores were developed during the past few years [4, 15, 16], while such a substantial collection of approaches is not completely available for zeolites with the low Si/Al molar ratio of 1.0–1.5 (zeolite A and X). Up to present, only few papers referring to low-silica zeolites are published. Ryoo’ group has creatively used silanising chemicals as the mesopore-directing agent to synthesise mesoporous zeolites LTA [13]. Afterwards, Schwioger’s group demonstrated a synthesis method using same organosilane template to create mesoporous zeolite X [17], obtaining the new hierarchical zeolite X assemblies consists of ball-shaped house-of-cards-like nanosheets with intracrystal mesopores with an external surface area of $130\text{ m}^2\text{g}^{-1}$ and a mesoporous volume of $0.20\text{ cm}^3\text{g}^{-1}$, while the Brunauer–Emmett–Teller (BET) surface area is $724\text{ m}^2\text{g}^{-1}$. Lee *et al.* [18] demonstrated that the controlled decationisation of NaX zeolite can produce hierarchically micro/mesoporous zeolites with systematically variable micro and mesoporosity in which the secondary mesoporosity increased up to $0.18\text{ cm}^3\text{g}^{-1}$ at the cost of initial

microporosity while maintaining the total pore volume ($>0.41\text{ cm}^3\text{g}^{-1}$) and BET surface area ($>630\text{ m}^2\text{g}^{-1}$). Also, based on the method proposed by our research group, zeolite A with intracrystal mesopores is synthesised using nanosilica functioned by phenylaminopropyl-trimethoxysilane as a silicon source by means of a *bond-blocking* effect of hydrophobic organic group linked to the zeolite framework in synthesis [19].

According to the *bond-blocking* principle, we try to prepare a zeolitic material with the ordered mesoporous structure. In this Letter, pre-organofunctionalised mesoporous silica is used as the silicon source for the synthesis of mesoporous X zeolite with high external surface area and high microporous surface area. The structural characteristics of the meso-zeolite X are investigated and compared with microzeolite X.

2. Experimental section

2.1 Functionalisation of mesoporous silica: Mesoporous silica was functionalised by TPOAC (dimethyloctadecyl [3-(trimethoxysilyl) propyl] ammonium chloride, 72% wt% methanol solution, Aldrich) and defined as silanised mesosilica. A total of 30 g mesoporous silica was added into 600 ml of distilled water, and then 36 ml TPOAC in methanol solution was added into the former system. After refluxing for 8 h at 373 K, the silanised mesosilica was washed with ethanol several times, and then dried at 393 K.

2.2 Synthesis of mesoporous zeolite X: Mesoporous zeolite X was hydrothermally synthesised by using silanised mesosilica as the silicon source according to molar composition: $5\text{ Na}_2\text{O}:\text{Al}_2\text{O}_3:4\text{ SiO}_2:180\text{ H}_2\text{O}$. In the synthesis process, NaOH was dissolved in H_2O , in which solid silanised mesosilica was added under stirring. After the mixture was stirred for 1 h, sodium aluminate solution was added into the mixture and stirred continuously for 3 h. Then, 5 vol.% of the zeolite X directing agent was added. The resulting gel was transferred into an autoclave for crystallisation at 348 K for 5 d. The obtained powder was collected by filtration, washed and dried at 393 K, and then calcined at 823 K to remove the organic group. The calcined sample was further hydrothermally treated in deionised water at 373 K for 24 h under vigorous stirring. The eventually obtained sample is denoted as meso-NaX. A reference sample (mico-NaX)

was synthesised in the same approach as described above, only non-silanised mesosilica was used as the silicon source.

2.3 Characterisation of samples: Scanning electron microscope (SEM) images were obtained with the electron microscope Hitachi S-4800II FE-SEM. Transmission electron microscope (TEM) images were obtained in a JEOL JEM-1011. Nitrogen adsorption/desorption isotherms were conducted at 77 K in a Quantachrome Quadrasorb SI. Prior to the measurements, the samples were outgassed for 3 h at 573 K under vacuum. Adsorption isotherm of p-xylene was carried out on a Hiden Intelligent Gravimetric Analyser (IGA-002) instrument.

3. Results and discussion: The X-ray diffraction (XRD) patterns of mesoporous silica, silanised mesosilica, meso-NaX and micro-NaX (Figure S1) show that the silanised mesosilica sample preserves well-defined (100) peak of the ordered mesostructure in low-angle XRD (LXRD), and the peak position shifts to a higher angle compared with non-silanised mesosilica, mirroring the decreased pore size. During the hydrothermal synthesis of meso-zeolite X, the peaks at LXRD gradually disappeared, the amorphous mesosilica evolved to well-crystallised FAU zeolite. The meso-NaX and micro-NaX have the normal FAU-zeolitic structure, no other crystalline phase or amorphous silica is observed. The meso-NaX shows some broadening of the diffraction peaks and relatively weak intensity as compared with the micro-NaX demonstrates smaller crystalline size of the zeolitic particles.

The N_2 adsorption/desorption isotherms of micro-NaX and meso-NaX are given in Fig. 1. The high starting point of nitrogen adsorption at p/p_0 of 0.03 shows the filling of micropores of micro-NaX and meso-NaX at even lower pressure. Micro-NaX shows a usual type I isotherm of microporous structure. While for meso-NaX, the uptake of nitrogen shows a significant increase with pressure between 0.03 and 0.9, and a jump of nitrogen uptake is observed above 0.9. A pronounced hysteresis loop between 0.45 and 0.9 is also observed. This type IV isotherm is attributed to the capillary condensation of N_2 gas in mesoporous, indicating the presence of mesoporosity in the meso-NaX sample. A pore size distribution in Fig. 1 (insert) shows clearly the mesopore sizes of the meso-zeolite X are mainly between 3.5 and 15 nm centred 6.5 nm. The structural parameters of the zeolitic material in Table 1 indicate a considerable external surface area ($247 \text{ m}^2\text{g}^{-1}$) and mesopore volume ($0.44 \text{ cm}^3\text{g}^{-1}$), and high BET surface area ($991 \text{ m}^2\text{g}^{-1}$) and large total pore volume ($0.71 \text{ cm}^3\text{g}^{-1}$), as well as a high hierarchy factor. The data are far higher than these reported in public [17, 18].

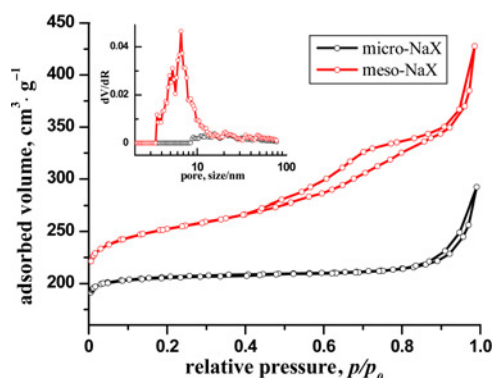


Fig. 1 N_2 adsorption/desorption isotherms of micro-NaX and meso-NaX samples and corresponding DFT pore size distribution derived from the adsorption branch

Table 1 Pore structure parameters of zeolite micro- and meso-NaX

| Samples | S_{BET}^a m^2g^{-1} | S_{mic}^b m^2g^{-1} | S_{ext}^c m^2g^{-1} | V_{mic}^d cm^3g^{-1} | V_{meso}^e cm^3g^{-1} | HF ^f |
|-----------|---|---|---|--|---|-----------------|
| micro-NaX | 848 | 815 | 33 | 0.30 | 0.15 | 0.03 |
| meso-NaX | 991 | 744 | 247 | 0.27 | 0.44 | 0.10 |

^aBET surface area

^bMicropore surface area

^cExternal surface area (t-plot method)

^dMicropore volume (t-plot method)

^eMesopore volume (total pore volume at $p/p_0 = 0.99 - V_{\text{mic}}$)

^fHierarchy factor (HF) = $(V_{\text{mic}}/V_{\text{Total}}) \times (S_{\text{ext}}/S_{\text{BET}})$ [20]

SEM and TEM images have been collected to examine the morphology and the pore structure of the two zeolites. As seen in Fig. 2 (top), the morphology of meso-NaX is very different from that of micro-NaX. The micro-NaX has a typical compact octahedral morphology of FAU zeolite crystallites with the smooth surface and clear crystalline edges. Whereas, the SEM images of meso-NaX at low magnification display the uniform aggregates with average particle size of ~600–1000 nm. At high magnification, it seems that each discrete aggregates is made up from stacked three-dimensional intergrowths of rectangular nanocrystals with the size of 60–80 nm × 400–500 nm. These images also show mesoporous voids between the primary particles. Elemental analysis from electron probe microanalysis gives a Si/Al molar ratio of 1.3 for both micro-NaX and meso-NaX. The high magnification TEM images (Fig. 2 bottom) further reveal that the aggregates were made of rectangular nanocrystals and the voids are created between nanocrystallites to form additional mesoscale porosity. In addition, surprisingly, the lattice fringes and mesoporosities are cleanly observed inside nanocrystals, indicating the preservation of microporous structures and the presence of intramesoporosity. These results agree well with the Density Functional Theory (DFT) pore size distribution derived from N_2 adsorption isotherms.

The used mesosilica has abundant hydroxyl species which can be functionalised by using organosilanes (see Figure S2: TG results of silanised mesosilica and as-synthesised micro-NaX). In the synthesis process, the hydrophobic moieties linked to Si atoms through Si–C covalent bonds partially block the growth of the zeolite units and crystals, resulting in the formation of nanosized zeolite and intracrystalline defect sites inside the nanocrystals [21]. After calcinations, the organic moieties covalently linked to the zeolite framework through Si–C bonds are removed, producing the

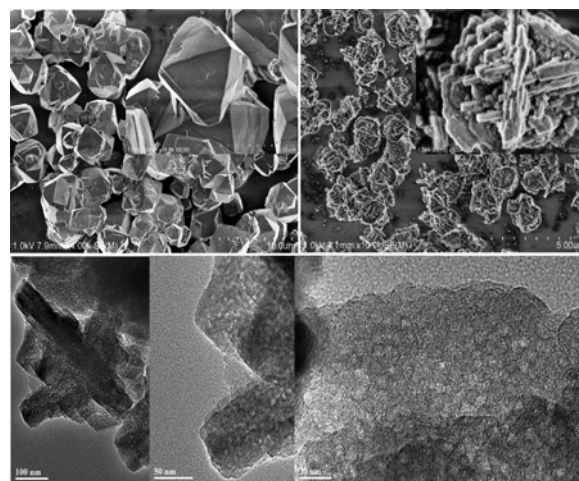


Fig. 2 SEM images of micro-NaX (top left) and meso-NaX (top right), and TEM images of meso-NaX (bottom)

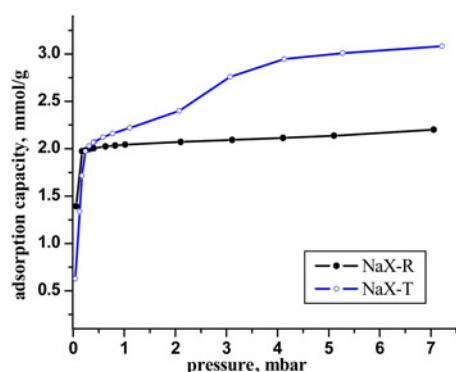


Fig. 3 Adsorption isotherms of *p*-xylene on micro-NaX and meso-NaX at 298 K

intracrystalline and intercrystalline mesopore in zeolite [19]. The mesoporous structure and high surface area of the mesosilica as a precursor are a key factor for obtaining the meso-NaX zeolite. The ordered mesoporous structure of the mesosilica destroys entirely itself on the eve of absolutely crystallisation of the zeolite.

To survey further pore structure and adsorption functions for organic compound of mesoporous zeolite X, the adsorption isotherms of *p*-xylene, which is an important chemical in the production of fibre and plastic bottles, on microporous micro-NaX and mesoporous meso-NaX at 298 K are examined, as shown in Fig. 3. Micro-NaX displays a typical type I isotherm, that is, the most of adsorption takes place in lower pressure, which indicates the presence of only micropore adsorption. Whereas, the adsorption of *p*-xylene on meso-NaX presents a continual increase with increasing pressure, after a very steep increase within lower pressure, which can be ascribed to adsorption on mesoporous and external surface of crystals, though the adsorption capacity is lower on meso-NaX than that on micro-NaX at even lower pressure, due to its smaller micropore volume relative to micro-NaX. This phenomenon proves again the presence of mesopores inside meso-NaX sample. At relative higher pressure, meso-NaX exhibits a much more adsorption capacity for *p*-xylene compared with micro-NaX. For example, meso-NaX has adsorption capacities of 2.4 and 2.9 mmol/g at the pressures of 2.1 and 4.1 mbar, respectively, which are higher than 2.1 mmol/g of meso-NaX at the same conditions. Therefore, with the same amounts of mass, meso-NaX can capture more *p*-xylene than micro-NaX. Conclusively, the introduction of mesopores into zeolite provides larger room for adsorbate, resulting in the enhancement of the adsorption capacity for adsorbates.

4. Conclusion: By using pre-organofunctionalised mesosilica as the silicon source, mesoporous zeolite X with considerably high total and external surface areas, as well as pore volumes, is hydrothermally synthesised. The characterisation results display that the meso-zeolite persist the inherent FAU structure, but different crystallographic morphology and pore structure compared with typical zeolite X, which is consisting of rectangular nanocrystal aggregates with the mesopores distributed over the entire domain of zeolite crystals. The formation of mesoporosities is ascribed to the ordered mesoporous structure of mesosilica and the incorporation of the hydrophobic moiety of organosilane into the framework of zeolite through a Si–C covalent bond blocking the growth of the zeolite units, resulting in the formation of nanosized zeolite and intracrystalline

mesopores. This mesoporous zeolite presented a higher mesopore volume and external surface area, and hence showed a larger adsorption capacity for *p*-xylene at relative higher pressure, being a practical industrial adsorbent in ion-exchange and adsorption separation.

5. Acknowledgments: This work was financially supported by the National Nature Science Foundation of China (grant nos. 51272169, U1463209).

6 References

- [1] Corma A.: 'Inorganic solid acids and their use in acid-catalyzed hydrocarbon reactions', *Chem. Rev.*, 1995, **95**, pp. 559–614
- [2] Vermeiren W., Gilson J.P.: 'Impact of zeolites on the petroleum and petrochemical industry', *Top. Catal.*, 2009, **52**, pp. 131–1161
- [3] Verhoef M.J., Kooyman P.J., van der Waal J.C., *ET AL.*: 'Partial transformation of MCM-41 material into zeolites: formation of nanosized MFI type crystallites', *Chem. Mater.*, 2001, **13**, pp. 683–687
- [4] Liu B., Chen F., Zheng L.: 'Synthesis and structural properties of hierarchically structured aluminosilicates with zeolite Y (FAU) frameworks', *RSC Adv.*, 2013, **3**, pp. 15075–15084
- [5] Wang B., Ma H.Z.: 'Factors affecting the synthesis of micro-sized NaY zeolite', *Microporous Mesoporous Mater.*, 1998, **25**, pp. 131–136
- [6] Lassinanti M., Hedlund J., Sterte J.: 'Faujasite-type films synthesized by seeding', *Microporous Mesoporous Mater.*, 2000, **38**, pp. 25–34
- [7] Egeblad K., Christensen C.H., Kustova M., *ET AL.*: 'Templating mesoporous zeolites', *Chem. Mater.*, 2008, **20**, pp. 946–960
- [8] Verboekend D., Perez-Ramirez J.: 'Desilication mechanism revisited: highly mesoporous all-silica zeolites enabled through pore-directing agents', *Chem. Eur. J.*, 2011, **17**, pp. 1137–1147
- [9] Groen J.C., Moulijn J.A., Perez-Ramirez J.: 'Desilication: on the controlled generation of mesoporosity in MFI zeolites', *J. Mater. Chem.*, 2006, **16**, pp. 2121–2131
- [10] Jacobsen C., Madsen C., Houzvicka J., *ET AL.*: 'Mesoporous zeolite single crystals', *J. Am. Chem. Soc.*, 2000, **122**, pp. 7116–7117
- [11] Tao Y., Kanoh H., Kaneko K.: 'Uniform mesopore-donated zeolite Y using carbon aerogel templating', *J. Phys. Chem. B*, 2003, **107**, pp. 10974–10976
- [12] Choi M., Na K., Kim J., *ET AL.*: 'Stable single-unit-cell nanosheets of zeolite MFI as active and long-lived catalysts', *Nature*, 2009, **461**, pp. 246–249
- [13] Choi M., Cho H.S., Srivastava R., *ET AL.*: 'Amphiphilic organosilane-directed synthesis of crystalline zeolite with tunable mesoporosity', *Nat. Mater.*, 2006, **5**, pp. 718–723
- [14] Cho K., Cho H.S., De Menorval L.C., *ET AL.*: 'Generation of mesoporosity in LTA zeolites by organosilane surfactant for rapid molecular transport in catalytic application', *Chem. Mater.*, 2009, **21**, pp. 5664–5673
- [15] Lopez-Orozco S., Inayat A., Schwab A., *ET AL.*: 'Zeolitic materials with hierarchical porous structures', *Adv. Mater.*, 2011, **23**, pp. 2602–2615
- [16] Hua Z.L., Zhou J., Shi J.L.: 'Recent advances in hierarchically structured zeolites: synthesis and material performances', *Chem. Commun.*, 2011, **47**, pp. 10536–10547
- [17] Inayat A., Knoke I., Spiecker E.: 'Assemblies of mesoporous FAU-type zeolite nanosheets', *Angew. Chem. Int. Ed.*, 2012, **51**, pp. 1962–1965
- [18] Lee S., Kim H., Choi M.: 'Controlled decationization of X zeolite: mesopore generation within zeolite crystallites for bulky molecular adsorption and transformation', *J. Mater. Chem. A*, 2013, **1**, pp. 12096–12102
- [19] Xue Z., Ma J., Hao W., *ET AL.*: 'Synthesis and characterization of ordered mesoporous zeolite LTA with high ion exchange ability', *J. Mater. Chem.*, 2012, **22**, pp. 2532–2538
- [20] Pérez-Ramirez J., Verboekend D., Bonilla A., *ET AL.*: 'Zeolite catalysts with tunable hierarchy factor by pore-growth moderators', *Adv. Funct. Mater.*, 2009, **19**, pp. 3972–3979
- [21] Jones C.W., Tsuji K., Davis M.E.: 'Organic-functionalized molecular sieves as shape-selective catalysts', *Nature*, 1998, **393**, pp. 52–54